



Validation of Moving-Overset 6-DOF Algorithm for Gas-Granular Two-Phase Flows

Dr. Raymond Fontenot^{*1}
Dr. Manuel Gale¹



2022 Workshop

Copyright © 2022 by Dr. Raymond Fontenot. Published by the NETL, with permission.

*** Primary/Corresponding Author
1: CFD Research**

g Mesh/Overset Capabilities for Accurate Cratering Simulations



between

Impact and plume impingement is a tightly coupled process

- Trajectory variation/pitch/attitude control can greatly modify rate and orientation of crater formation and evolution
- Surface erosion and debris trajectory pose significant risks to manned and unmanned vehicles and in-situ assets (surface material can reach 10 km/s speeds!)
 - Non-orthogonal landings increase risks
- PSI validation data currently limited to stationary (but varying heights) [1]
- Validation data at impact speeds ≤ 5 m/s is limited (Apollo 14 landed at ~ 4.3 m/s)



Figure 1. (left) LEM camera views from Apollo 15 landing showing progression of plume-regolith interaction resulting in high-speed particle sheets obscuration. [1](right) Regolith dust cloud formation during Morpheus lander plume impinging on Mars simulant[2].



Figure 2. MSL Skycrane plume induced surface cratering[3].

[1] Diaz-Lopez, M. X., Gorman, M., Rubio, J. S., and Ni, R., "Plume-surface Interaction Physics Focused Ground Test 1: Diagnostics and Preliminary Results," *AIAA Scitech 2022 Forum*, 2022, p. 1810.



Overview of Presentation

- Governing Equations
- Overset Methodology
- Moving Mesh Methodology
- Verification Cases
 - Theodorsen Plunging Airfoil (gas-only)
 - Houim Shocktube
- Seguin Sphere Drop Validation Study
 - Comparisons of 3 Granular Pressure Models
 - Comparisons of Full-Slip to No-Slip Wall Boundary Conditions

Governing Equations: Overview

Unstructured Finite Volume:

$$\frac{\partial}{\partial t} \int_{\Omega} H_c dV + \int_{\partial\Omega} (F_i - F_v) \cdot \vec{n} dS = \int_{\Omega} F_{source} dV$$

-Real Gas Species
-Mixed gas-granular continuity
-Gas Momentum
-Gas Energy

$$F_i = \begin{bmatrix} \alpha_g \rho_g Y_{g,0} \vec{u}_g \\ \vdots \\ \alpha_g \rho_g Y_{g,Ng-1} \vec{u}_g \\ \alpha_g (\rho_g \vec{u}_g \otimes \vec{u}_g + p_g \vec{I}) \\ \alpha_g (\rho_g e_{g,0} + p_g \vec{I}) \vec{u}_g \\ \alpha_s \rho_s Y_{s,0} \vec{u}_s \\ \vdots \\ \alpha_s \rho_s Y_{s,Ns-1} \vec{u}_s \\ \alpha_s (\rho_s \vec{u}_s \otimes \vec{u}_s + p_s \vec{I}) + p_s \vec{I} \\ [\alpha_s (\rho_s e_{s,0} + p_s \vec{I}) + p_s \vec{I}] \vec{u}_s \\ 1.5 \alpha_s \rho_s \Theta \vec{u}_s \end{bmatrix}, F_v = \begin{bmatrix} \alpha_g \rho_g Y_{g,0} \vec{V}_{g,0} \\ \vdots \\ \alpha_g \rho_g Y_{g,Ng-1} \vec{V}_{g,Ng-1} \\ 0 \\ \overline{\tau}_g - \overline{\tau}_{g,t} \\ \vec{u}_g \cdot (\overline{\tau}_g - \overline{\tau}_{g,t}) + \vec{q}_g + \sum_{i=1}^{Ng} \rho_g h_g V_{g,i} \\ \alpha_s \rho_s Y_{s,0} \vec{V}_{s,0} \\ \vdots \\ \alpha_s \rho_s Y_{s,Ns-1} \vec{V}_{s,Ns-1} \\ 0 \\ \overline{\tau}_s + \frac{\alpha_s}{\alpha_g} (\overline{\tau}_g - \overline{\tau}_{g,t}) \\ \vec{u}_s \cdot \left(\overline{\tau}_s + \frac{\alpha_s}{\alpha_g} (\overline{\tau}_g - \overline{\tau}_{g,t}) \right) + \vec{q}_s + \sum_{i=1}^{Ng} \rho_s h_s V_{s,i} \\ \kappa \nabla \Theta \end{bmatrix}$$

$$H_c = [\alpha_g \rho_g Y_{g,0}, \dots, \alpha_g \rho_g Y_{g,Ng-1}, \alpha_g \rho_g + \alpha_s \rho_s, \alpha_g \rho_g \vec{u}_g, \alpha_g \rho_g e_{g,0}, \alpha_s \rho_s Y_{s,0}, \dots, \alpha_s \rho_s Y_{s,Ns-1}, \alpha_s \rho_s, \alpha_s \rho_s \vec{u}_s, \alpha_s \rho_s e_{s,0}, 1.5 \alpha_s \rho_s \Theta_s]^T$$

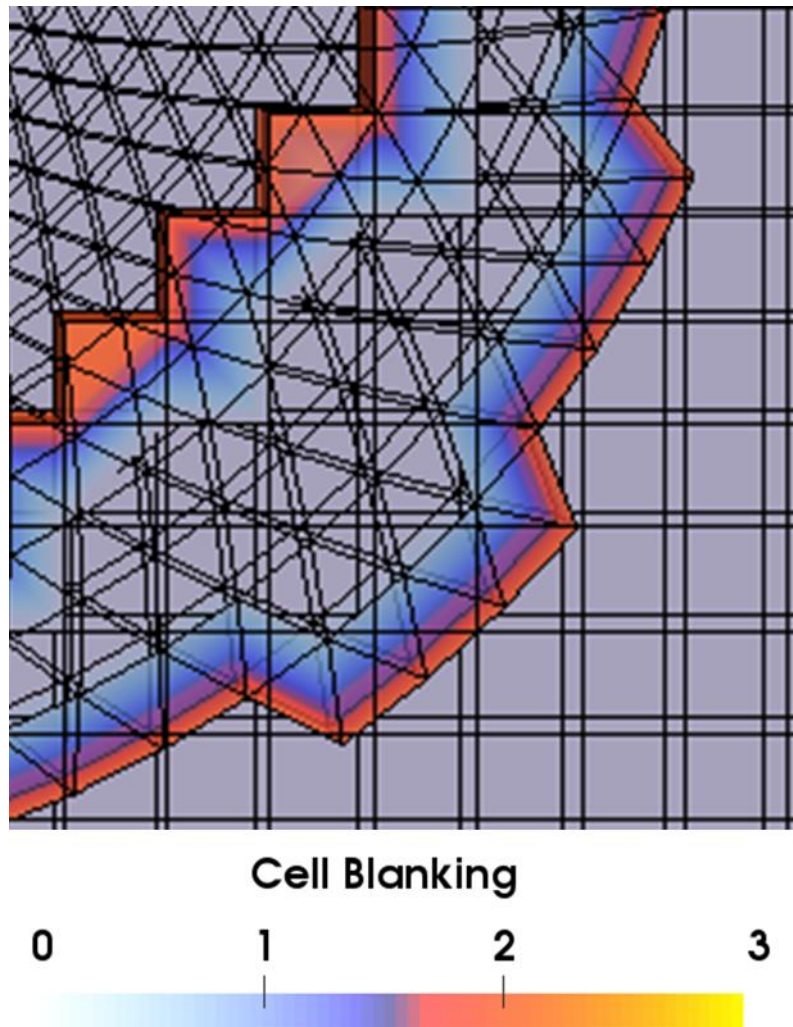


$$H_p = [Y_{g,0}, \dots, Y_{g,Ng-1}, P_g, \vec{u}_g, T_g, Y_{s,0}, \dots, Y_{s,Ns-1}, \alpha_s, \vec{u}_s, T_s, \Theta_s]^T$$



Overset Methodology

- Grids are merged and tagged in pre-processing step, with overset geometric region specified at input
- Geometric specification and nearest neighbor/KD-tree search defines cells for hole-cutting and interpolation/information exchange between meshes
- Cell blanking metrics for hole-cutting/interpolation:
 - 0: Standard cell used for interpolation purposes
 - 1: Standard cell not used for interpolation purposes
 - 2: Cell that receives information from interpolation donor cells
 - 3: Frozen cell that is not overlapping any other cell, or cell outside of physical domain
- 0 or 1 cells are solved normally
- 2 or 3 cells are interpolated from 0 cells and have solution data overridden
- At least 2 fringe (overlapping) cells required to avoid hole-cutting issues
- Boundary condition at interface is a Dirichlet boundary with values interpolated using second-order van Aldaba-limited upwinding



Moving Mesh Methodology

- Four types of motion supported: prescribed, six-degrees of freedom (6DOF), rotation, and stationary
- Geometric conservation law (GCL) [1] accounts for effect of moving mesh velocity (U_s)

$$g_{cl\pm} = (U_s \Delta S)_{L,R}$$

- GCL condition is removed as a source \mathbf{H}_R for the gas- and granular-phase states $\mathbf{Q}_{g,s}$

$$\mathbf{H}_R - = (\alpha \rho)_g g_{cl} \mathbf{Q}_g \quad \mathbf{H}_R - = (\alpha \rho)_S g_{cl} \mathbf{Q}_S$$

- GCL condition is also removed from source Jacobians

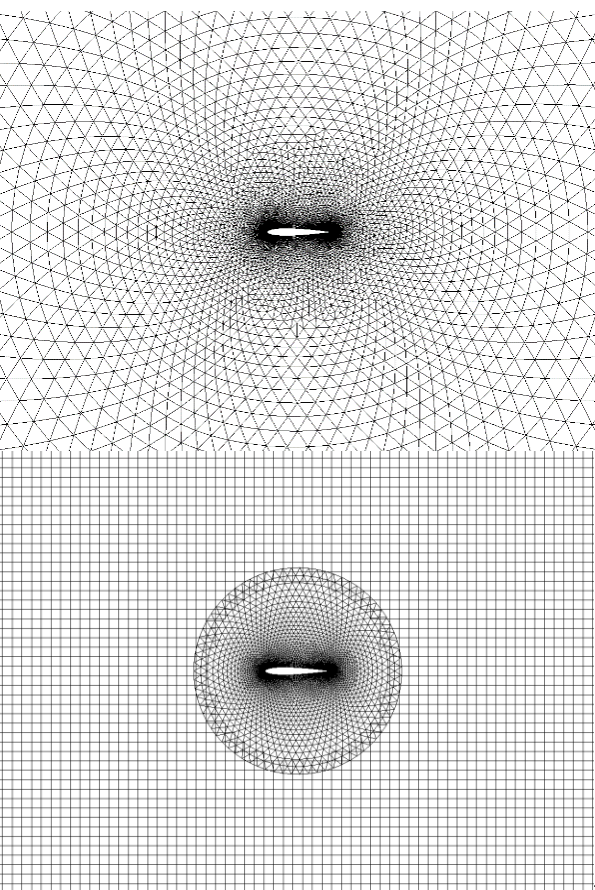
$$\mathbf{H}_{SD} - = g_{cl} \frac{d\mathbf{Q}}{d\mathbf{q}}$$

- For 6DOF, forces and torques on the surface of moving body are computed from contributions of gas- and granular-phase

$$F = F_I + F_V = (F_g + F_s)_I + (F_g + F_s)_V$$
$$T = T_I + T_V = (T_g + T_s)_I + (T_g + T_s)_V$$

Verification Cases: Theodorsen Airfoil

- Initial verification case of canonical gas-only Theodorsen Plunging Airfoil
- Comparison between theoretical, moving mesh, and overset-moving mesh
- Results for both moving mesh and overset-moving mesh compare favorably to theoretical values of lift coefficient



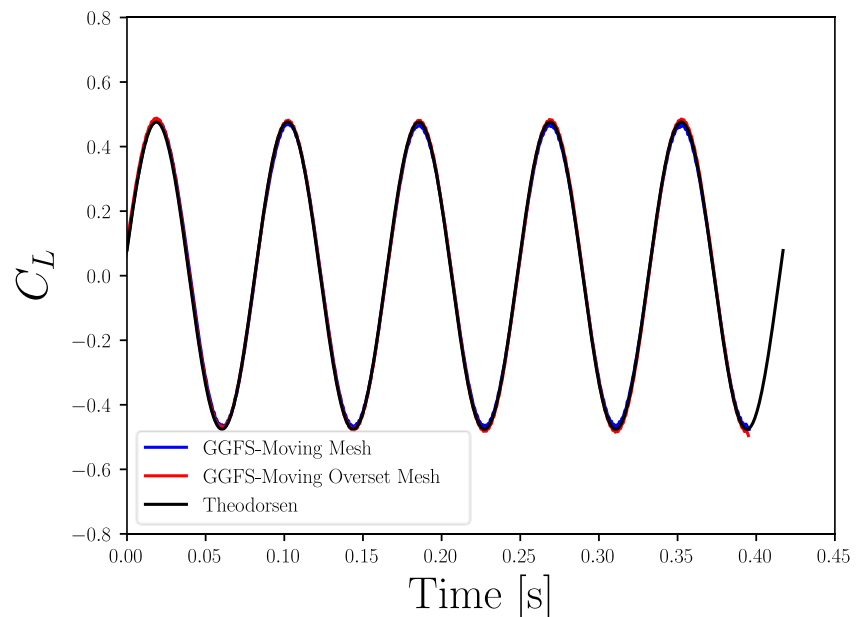
Original Mesh

Overset Mesh

$$h(t) = h_0 \sin(2\pi ft)$$

$$C_L = \frac{\pi c}{2U_\infty^2} \ddot{h} + \frac{2\pi}{U_\infty} C(k) \dot{h}$$

$$k = \frac{\pi c f}{U_\infty}$$



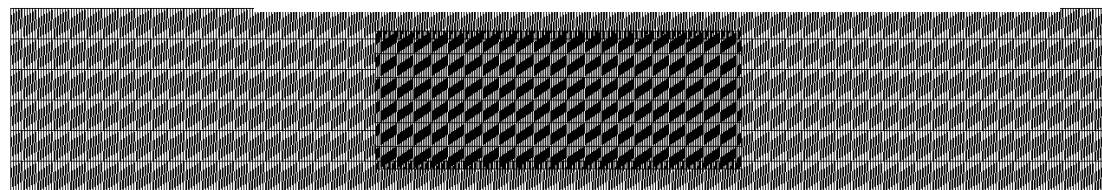
Verification Cases: Houim Shock Tube

- Houim shock tube case is utilized to verify gas-granular overset methodology
- Background mesh 6x600 nodes over $[(0,0), (0.6, 0.08)]$ m
- Overset mesh is moved diagonally over the background mesh from $(0.25, 0.04)$ to $(0.35, 0.06)$ linearly from an initial position of $[0.3, 0.5]$
- Simulation is performed for 1840 iterations at $dt = 1e-7$ s

Parameters for Houim Shock Tube Case [1]

Reference Pressure	p_{ref}	101325	Pa
Reference Density	ρ_{ref}	1.293	$\frac{\text{kg}}{\text{m}^3}$
Particle Diameter	d_s	10	μm
Particle Density	ρ_s	1470	$\frac{\text{kg}}{\text{m}^3}$
Driver Volume Fraction	α	0.4	-
Driver Pressure	$\frac{p}{p_{ref}}$	10	-
Driver Density	$\frac{\rho}{\rho_{ref}}$	10	-
Driver Velocity	$\frac{u}{u_{ref}}$	0	-
Test Section Volume Fraction	α	0	-
Test Section Pressure	$\frac{p}{p_{ref}}$	100	-
Test Section Density	$\frac{\rho}{\rho_{ref}}$	1	-
Test Section Velocity	$\frac{u}{u_{ref}}$	0	-
Specific Heat, Constant Pressure	C_p	987	$\frac{\text{J}}{\text{kg K}}$
Coefficient of Restitution	e	0.999	-

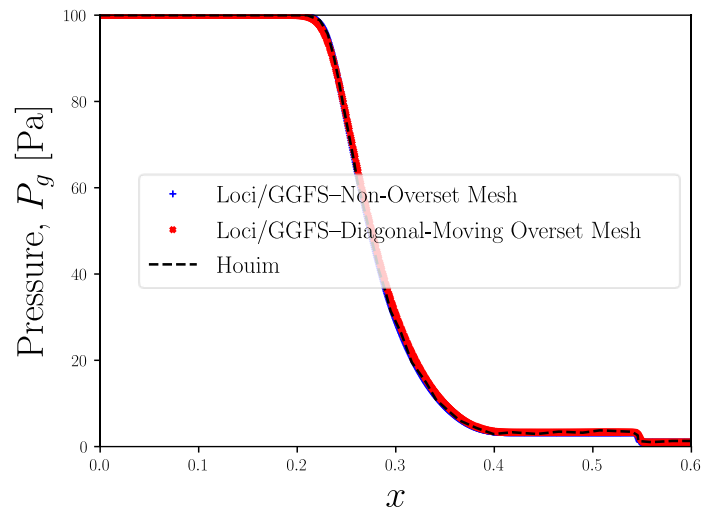
Mesh with
Overset Grid



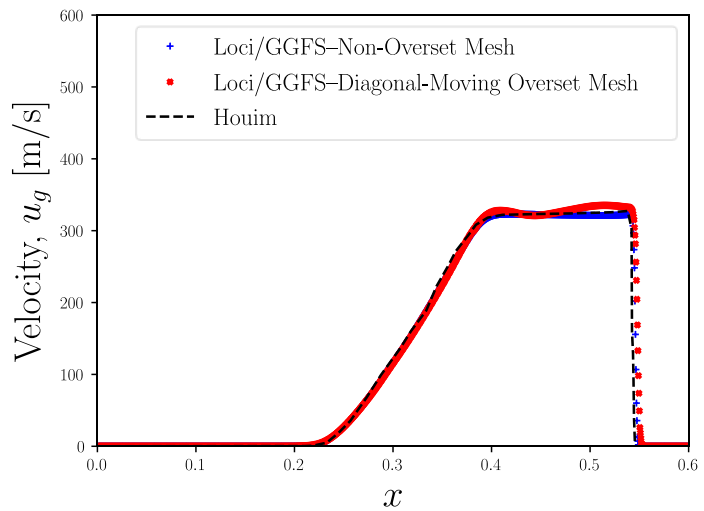
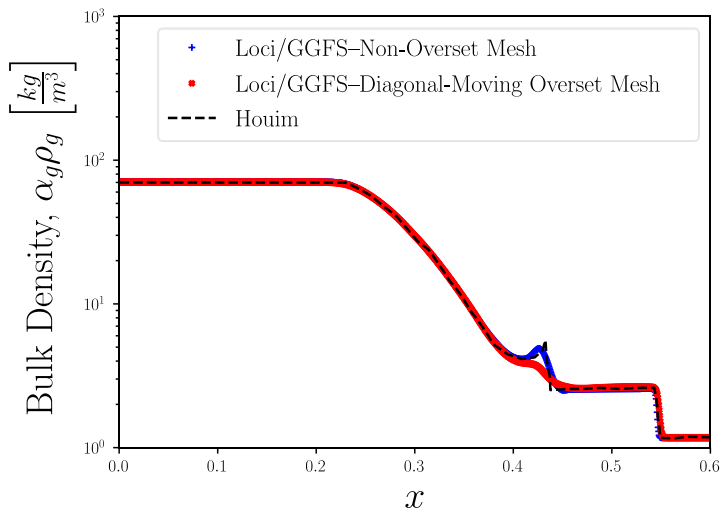
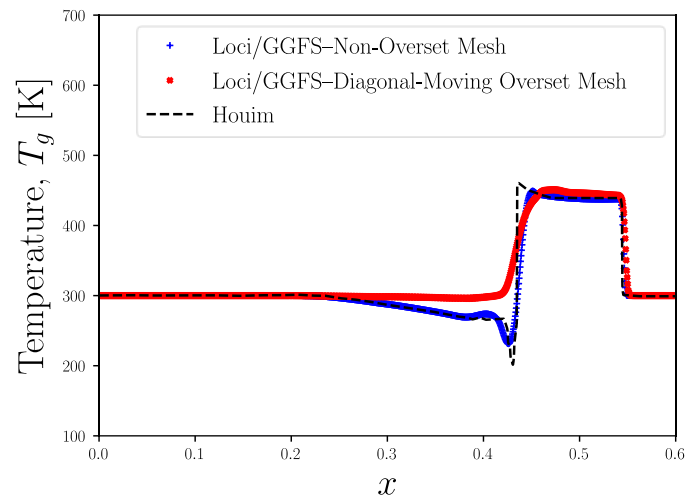
[1] Houim, R. W., and Oran, E. S., "A multiphase model for compressible granular-gaseous flows: formulation and initial tests," *Journal of fluid mechanics*, Vol. 789, 2016, p. 166.



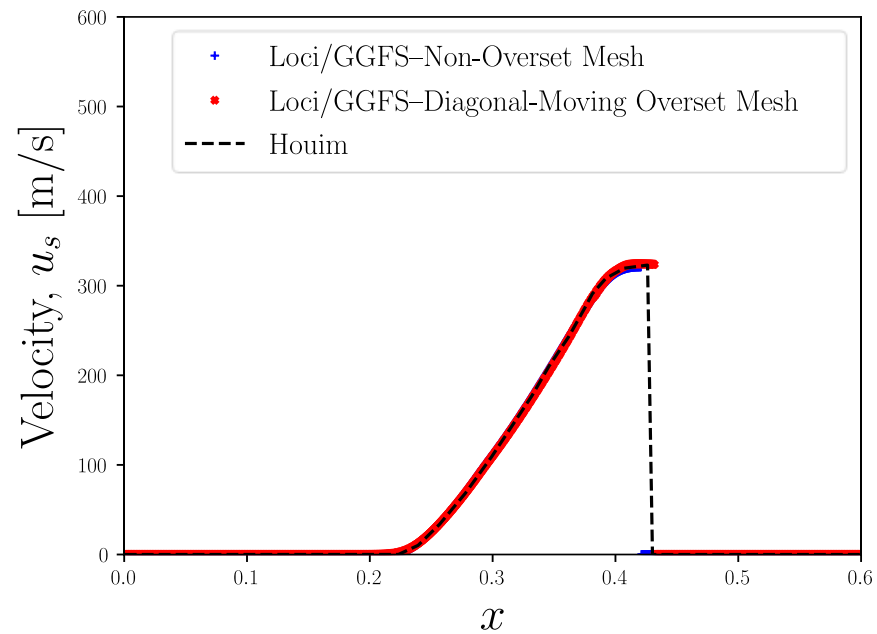
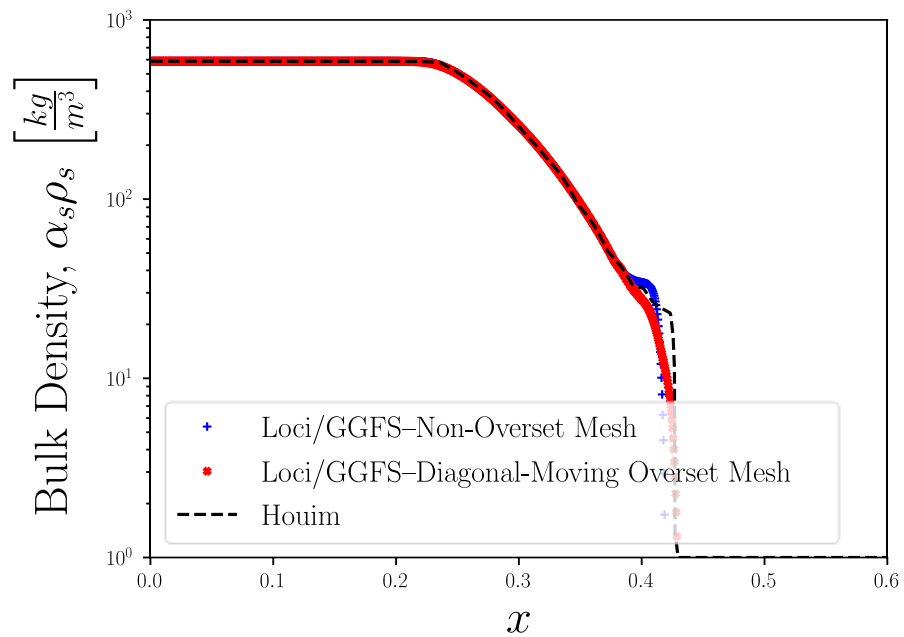
Verification Cases: Houim Shock Tube



Results compare
favorably to the
stationary mesh/no
overset case.



Verification Cases: Houim Shock Tube

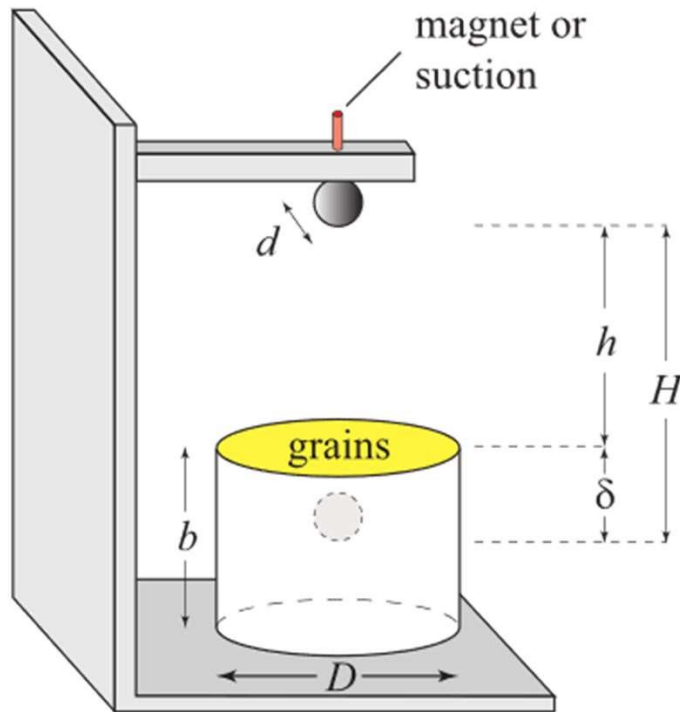


Results compare
favorably to the
stationary mesh/non-
overset case.



Seguin Sphere Drop Validation Case

Experimental Setup



- Steel sphere ($d = 5$ mm) dropped from various heights ($h=(0.05,0.5)$ m) and measured penetration depth (δ)
- Bin is wide enough (D) and deep enough (b) that wall effects of bin are negligible

The granular medium consists of glass beads ($\rho_s = 2500$ kg/m³) slightly polydisperse in size, with a diameter range of 300–400 μm . Before each drop, the granular medium is prepared by gently stirring the grains with a thin rod. The container is then overfilled and the surface levelled using a straight edge. We have checked that this preparation leads to reproducible results with only small variations. The grain size is much smaller than the falling sphere diameter so that the granular medium can be considered as a continuum medium. [1]

[1] Seguin, Antoine, Yann Bertho, Philippe Gondret, and Jérôme Crassous. "Sphere penetration by impact in a granular medium: A collisional process." *EPL (Europhysics Letters)* 88, no. 4 (2009): 44002.

Seguin Sphere Drop Validation Case

Numerical Setup

INSERT MESH
HERE

- 2D grid with overset sphere with 6DOF free-fall
- Free-slip and no-slip wall boundary conditions on sphere (partial-slip not verified/validated at time of study)
- 350 μm glass spheres in granular bed
- Simulations run until steady-state (the sphere is motionless in granular material)
- Laminar flow with hllcCT flux for gas- and granular-phase
- 2nd-order spatial (Venkatakrishnan limiter) and temporal (implicit, 10 newton iterations per time step, $\text{dt}=1\text{e-}6$ s) accuracy
- 3 granular pressures models tested
 - Srivastava [1]
 - Pengfei [2]
 - mu-Rheological [3]

[1] Srivastava, A., and Sundaresan, S., "Analysis of a frictional-kinetic model for gas-particle flow," *Powder technology*, Vol. 129, No. 1-3, 2003, pp. 72-85.

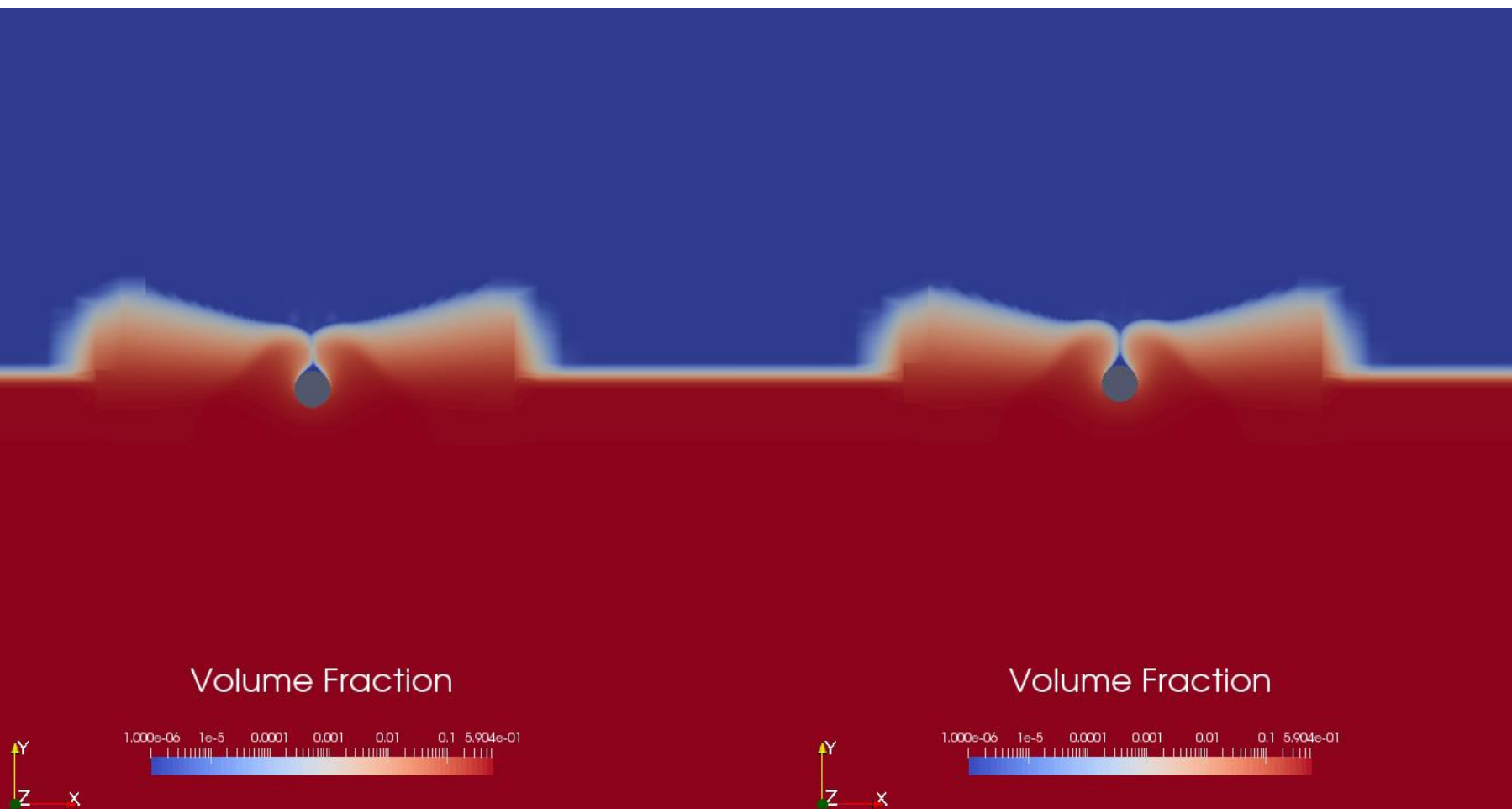
[2] Si, P., Shi, H., and Yu, X., "A general frictional-collisional model for dense granular flows," *Landslides*, Vol. 16, No. 3, 2019, pp. 485-496.

[3] Schneiderbauer, S., Aigner, A., and Pirker, S., "A comprehensive frictional-kinetic model for gas-particle flows: Analysis of fluidized and moving bed regimes," *Chemical Engineering Science*, Vol. 80, 2012, pp. 279-292.

Seguin Sphere Drop Validation Case

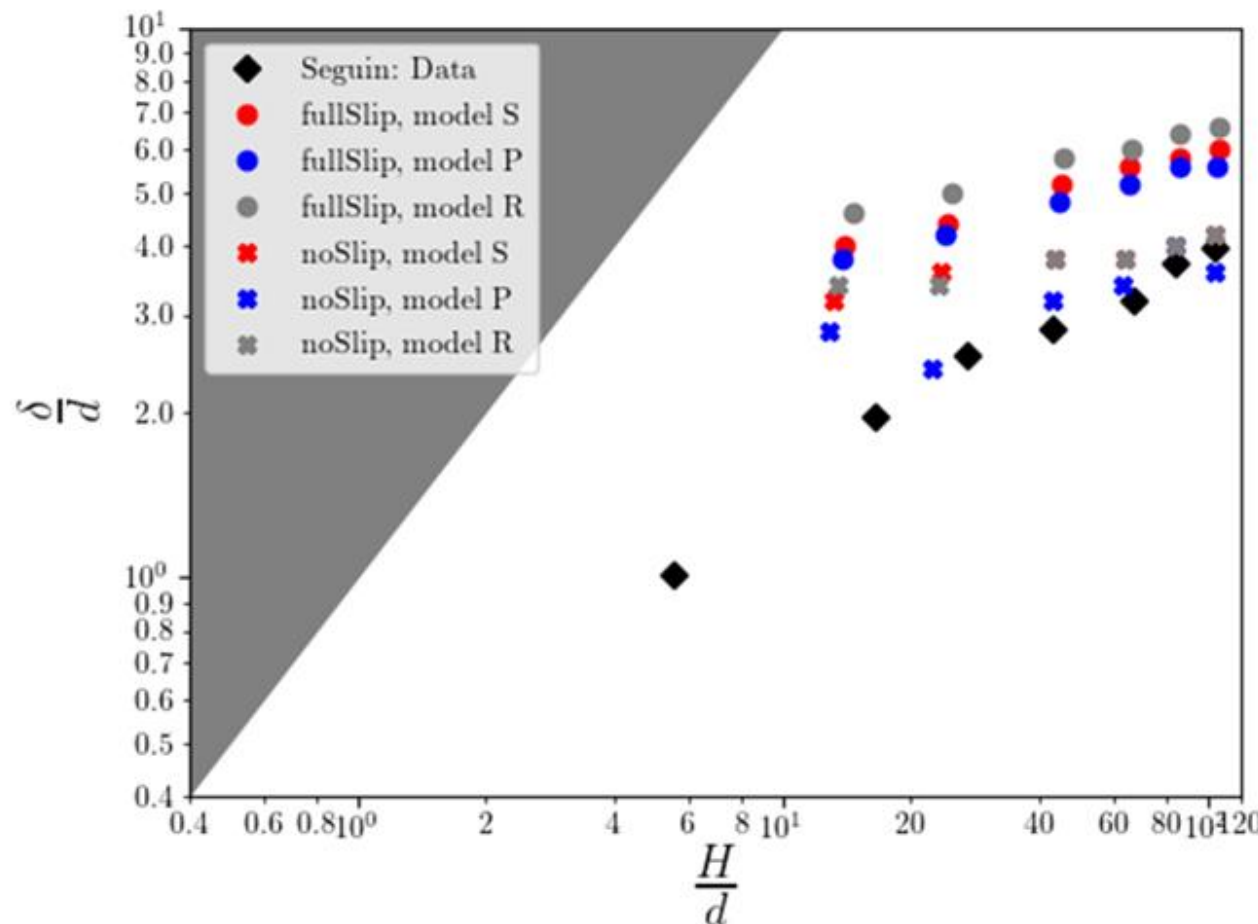
Full-Slip Boundary

No-Slip Boundary



Seguin Sphere Drop Validation Case

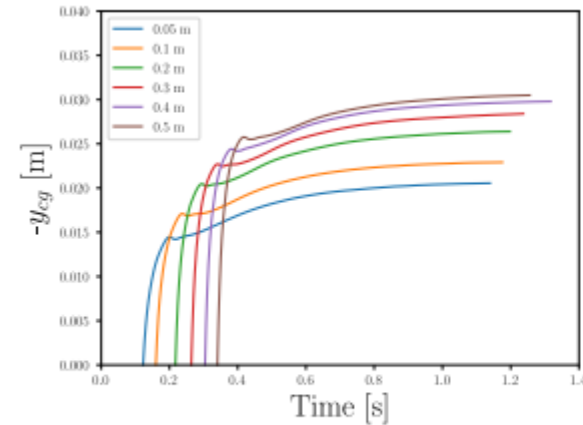
Normalized Penetration Depth



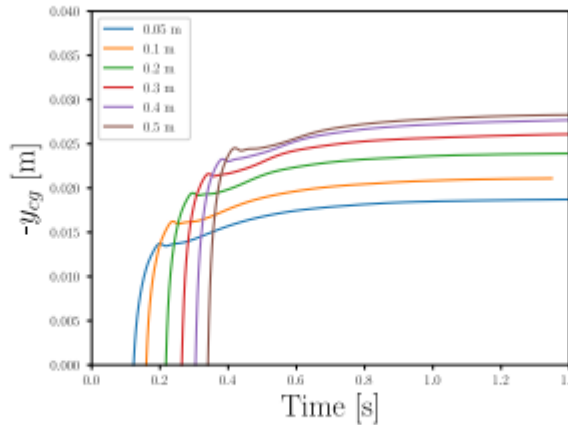
Seguin Sphere Drop Validation Case

Comparison of Trajectories

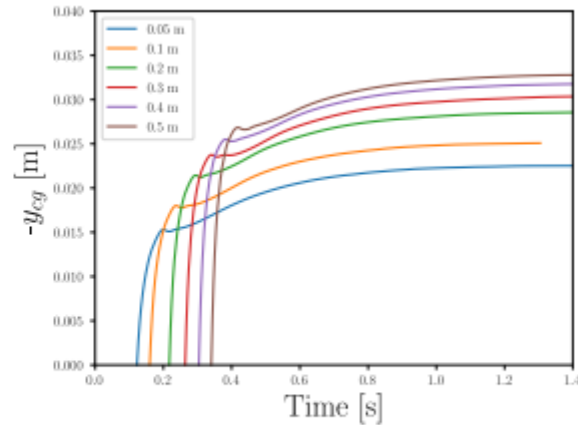
Full-Slip



(a) Srivastava

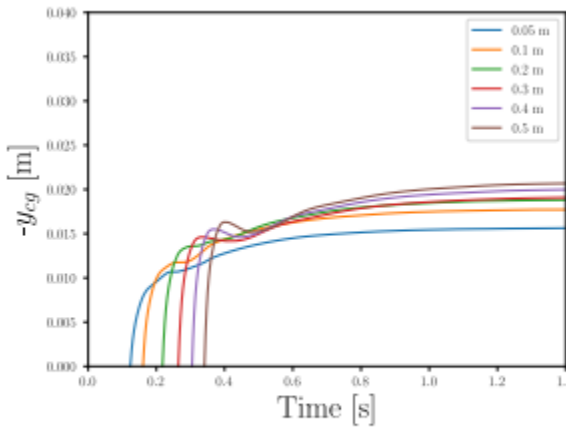


(b) Pengfei

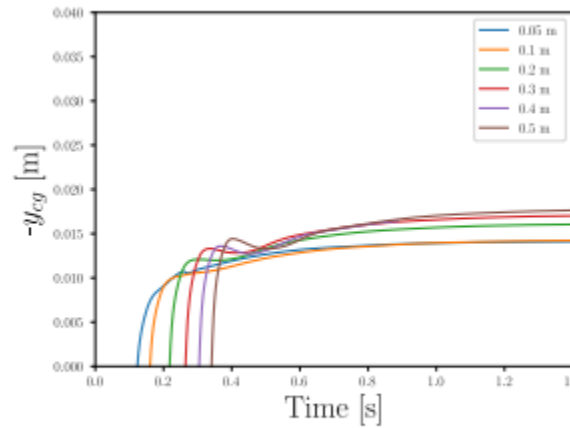


(c) mu-Rheology

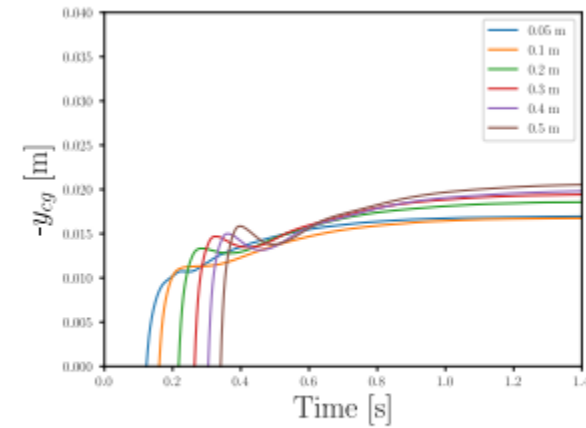
No-Slip



(a) Srivastava



(b) Pengfei



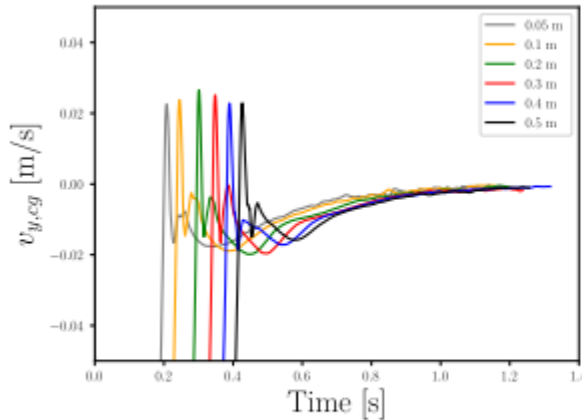
(c) mu-Rheology



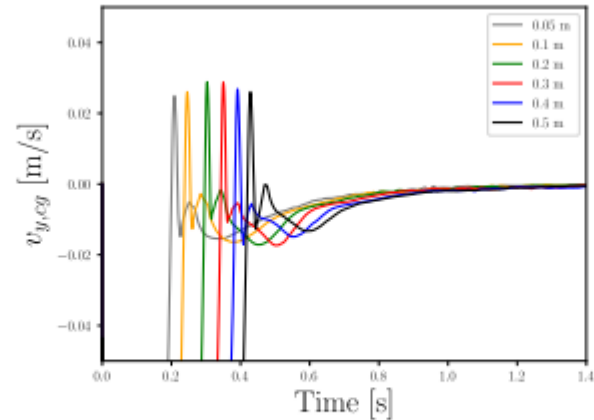
Seguin Sphere Drop Validation Case

Comparison of Velocities

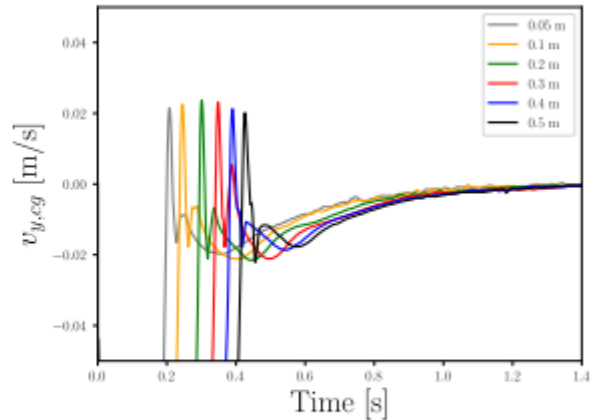
Full-Slip



(a) Srivastava

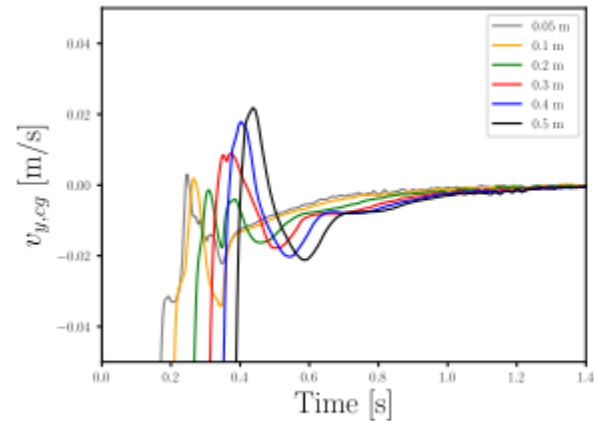


(b) Pengfei

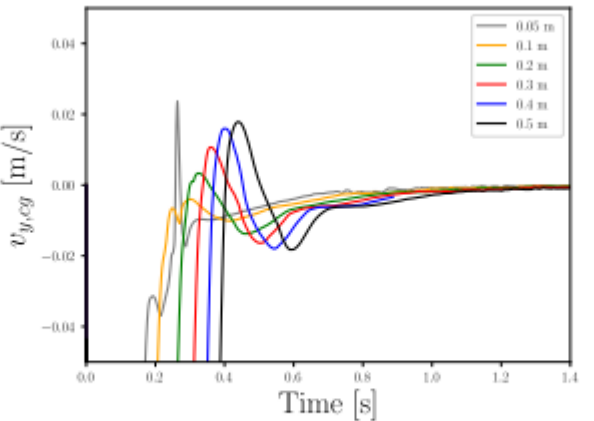


(c) mu-Rheology

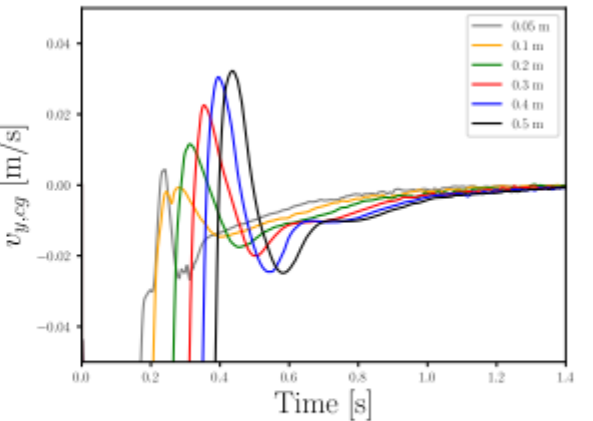
No-Slip



(a) Srivastava



(b) Pengfei



(c) mu-Rheology



Conclusions & Future Work

- Conclusions
 - Overset and moving mesh algorithms successfully implemented in Loci/GGFS
 - Verified for several gas-only and gas-granular cases (some not shown herein)
 - Loci/GGFS data compared favorably to Seguin data
 - No-slip results with Pengfei and mu-Rheological models closer to Seguin
 - Full-slip boundary condition on sphere results in greater penetration depths/higher velocities
 - Both boundary conditions (stronger in no-slip) clearly show rebound phenomena as granular bed is compressed
 - While boundary conditions presented herein ‘bound’ more realistic partial slip case, exact matching of experiment was not expected
- Future Work
 - Investigate partial slip wall of Schneiderbauer [1] with all granular pressure models presented herein
 - Comparison to DEM
 - Investigate effects of polydispersity of granular material on penetration

[1] Schneiderbauer, Simon, David Schellander, Andreas Löderer, and Stefan Pirker. "Non-steady state boundary conditions for collisional granular flows at flat frictional moving walls." International Journal of Multiphase Flow 43 (2012): 149-156.



Acknowledgements

- Worked performed under NASA SBIR Contract 80NSSC20C0032

